

# ***Polarization at Pt electrodes of a fuel cell with a high temperature-type proton conductive solid electrolyte***

H. UCHIDA, S. TANAKA, H. IWAHARA

*Department of Environmental Chemistry and Technology, Faculty of Engineering, Tottori University, Tottori 680, Japan*

Received 5 March 1984; revised 1 May 1984

The polarization phenomena of platinum electrodes in the high temperature-type proton conductor fuel cell were studied by means of a current interruption method. The polarization of the cathode could not be neglected below 900° C, whereas the polarization of the anode was negligibly small. The polarization resistance,  $R_p$ , at the cathode decreased with increasing oxygen partial pressure,  $P_{O_2}$  ( $R_p \propto P_{O_2}^{-1/4}$ ), and the activation energy for  $R_p$  was 0.99 eV. The rate determining step for the cathode reaction was considered to be the surface diffusion of adsorbed oxygen atoms on platinum to the electrochemically active site on the solid electrolyte.

## **1. Introduction**

The high temperature solid electrolyte fuel cell has been considered to be one of the promising direct energy converters of the future. The over-potential behaviour of the cell is of interest from both theoretical and practical viewpoints. Many investigators have studied the anodic and cathodic polarization phenomena at platinum or other noble metal electrodes on doped ceria [1-7], stabilized zirconia [6-17] or some perovskite-type oxides [18] by using various electrochemical methods. All the solid electrolytes for these studies are high temperature-type oxide ion conductors and, therefore, oxide ions take part in the electrode process of the cell reactions. Another candidate type of solid electrolyte for the fuel cell is the proton conductor in which protons take part in the electrode reactions.

Several years ago, we discovered high temperature-type proton conductive solid electrolytes based on  $SrCeO_3$  and fabricated a fuel cell using these as the diaphragm and porous platinum as the electrode material [19-22]. The cell worked stably at 800-1000° C. We confirmed that water vapour was produced at the air electrode on discharging the cell with the evolution rate corresponding to the theoretical rate calculated from Faraday's law. This fact indicates that the charge carrier in this

electrolyte is a proton (anode:  $H_2 \rightarrow 2H^+ + 2e$ ; cathode:  $2H^+ + 1/2O_2 + 2e \rightarrow H_2O$ ) and not an oxide ion; the oxide ion conductor cell must give water vapour at the fuel electrode (anode:  $O^{2-} + H_2 \rightarrow H_2O + 2e$ ; cathode:  $1/2O_2 + 2e \rightarrow O^{2-}$ ). Using the same electrolyte, we have demonstrated proton conduction in studies on a steam electrolysis cell for hydrogen production [19-21], a steam concentration cell [19, 23, 24] and a hydrogen concentration cell [25]. These cells could also be operated stably as expected. However, the polarization characteristics of platinum electrodes on the  $SrCeO_3$ -based electrolytes were not completely clear.

In this research, we studied the polarization phenomena at the interface between platinum electrodes and the  $SrCeO_3$ -based proton conductive solid electrolyte in the hydrogen fuel cell.

## **2. Experimental details**

The proton conductive solid electrolyte used in this study was  $SrCe_{0.95}Yb_{0.05}O_{3-\alpha}$ , where  $\alpha$  is the number of oxygen deficiencies per perovskite-type oxide unit cell. The preparation of the specimens was similar to that in the previous study [19] except that the sintering was carried out at about 1500° C for 10 h in air in order to obtain denser sinters. The sinters obtained were sliced into thin

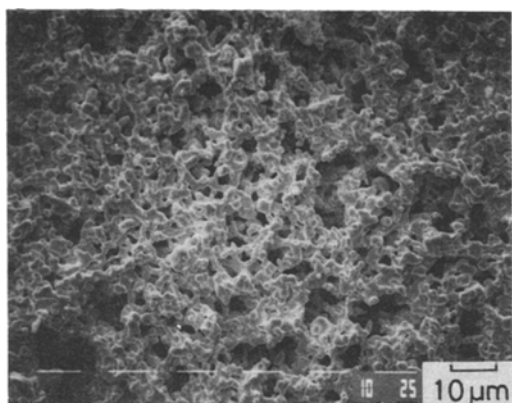


Fig. 1. SEM picture of the freshly prepared platinum electrode on the specimen disc.

discs (thickness: about 0.5 mm, diameter: 12 mm) to provide test specimens.

The construction of the solid electrolyte fuel cell was the same as in reference [21]. The electrode material used was platinum. In order to prepare the platinum paste, fine platinum powder obtained by the thermal decomposition of  $(\text{NH}_4)_2\text{PtCl}_6$  was suspended in *n*-butyl acetate. The platinum paste was smeared on both faces of the specimen electrolyte (projected area:  $0.5 \text{ cm}^2$ ) and fired at  $1000^\circ \text{C}$  in open air for 1 h.

Fig. 1 shows an SEM picture of the freshly prepared platinum porous electrode on the specimen surface. It can be observed that the electrode is porous and the platinum particles are fine and fairly uniform in size. The contact with the electrodes was made through a platinum grid to which platinum lead wires were attached. A platinum wire was wound around the side of the electrolyte disc as the reference electrode. The electrode compartments were separated by the specimen electrolyte and each electrode compartment was sealed by a glass ring packing.

Hydrogen gas saturated with water vapour at room temperature (vapour pressure  $P_{\text{H}_2\text{O}} = 17\text{--}20 \text{ Torr}$ ) was used as the anode gas. Air, oxygen or a mixture of oxygen and nitrogen with various oxygen partial pressures ( $P_{\text{O}_2}$ ) was used as the cathode gas in a wet state ( $P_{\text{H}_2\text{O}} = 17\text{--}20 \text{ Torr}$ ). The total pressure of both electrode gases was 1 atm ( $= 1.013 \times 10^5 \text{ Pa}$ ) in all cases. The  $P_{\text{O}_2}$  in the gases was measured by a concentration cell-type oxygen meter composed of stabilized zirconia (YSZ).

Polarization characteristics of the electrodes were studied by the current interruption method. A current pulse (pulse width: 0.1 ms, repeat time: 2 ms) was applied to the fuel cell from a current pulse generator (Hokuto Denko, Model HC-110). The transient behaviour of the electrode potential was measured by a high input impedance voltmeter (Hokuto Denko, Model HE-101A) and monitored by an oscilloscope (Hitachi, digital memory scope, Model VC-801-L).

### 3. Results and discussion

Using  $\text{SrCe}_{0.95}\text{Yb}_{0.05}\text{O}_{3-\alpha}$  as the solid electrolyte and porous platinum as the electrode material, a hydrogen–air fuel cell was constructed to operate at  $800\text{--}1000^\circ \text{C}$ . The cell worked stably as the previous cell did [19–22]. The e.m.f.s were close to the theoretical values and a steady and stable current could be drawn out. Fig. 2 shows the typical transient behaviour of the electrode potential on interrupting the discharge current. The

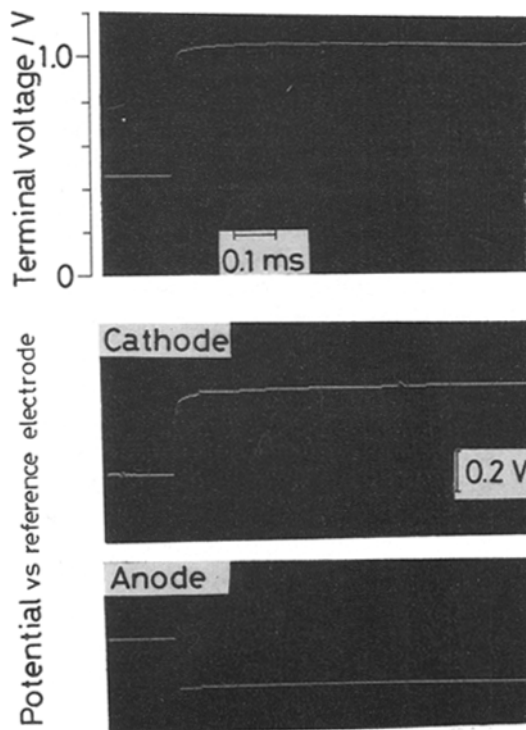


Fig. 2. Typical transient behaviour of the electrode potential on interrupting the discharge current.  $\text{H}_2$ , Pt |  $\text{SrCe}_{0.95}\text{Yb}_{0.05}\text{O}_{3-\alpha}$  | Pt, air. Temperature:  $900^\circ \text{C}$ ,  $i = 0.05 \text{ A cm}^{-2}$ .

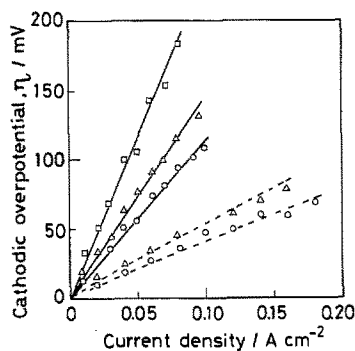


Fig. 3. Polarization characteristics of the platinum cathode in  $H_2$ -fuel cell. —:  $800^\circ C$ , - - - - :  $900^\circ C$   $P_{O_2}$  in the cathode gas (atm);  $\circ$ : 1.0,  $\Delta$ : 0.21,  $\square$ :  $1.71 \times 10^{-2}$ .

instantaneous voltage drop after the current interruption is taken as the  $iR$  drop. Since this  $iR$  drop is large compared to the residual voltage drop, the major limitation of this cell can be regarded as the resistance of the solid electrolyte as observed in the previous study. In this cell, the polarization of the anode ( $H_2$  electrode) was negligibly small in the whole temperature range examined. Therefore, the anodic reaction (injection of protons into the electrolyte) can be considered to occur reversibly. However, since the polarization at the cathode (air electrode) could not be neglected below  $900^\circ C$ , we studied the polarization phenomena for the cathode reaction ( $2H^+ + 1/2O_2 + 2e \rightarrow H_2O$ ).

Changing the partial pressure of oxygen ( $P_{O_2}$ ), the polarization curves at the cathode were measured by the interruption method and the results are shown in Fig. 3. The relation between the overpotential,  $\eta$ , and the current density is linear and the gradient of the line is steep at lower  $P_{O_2}$  and lower temperature. The polarization resistance,  $R_p$ , was calculated from the gradient of the line in Fig. 3 and plotted against the  $P_{O_2}$  in Fig. 4.

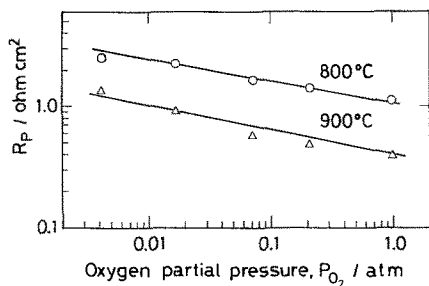


Fig. 4. Plot of  $R_p$  against  $P_{O_2}$  at the cathode.

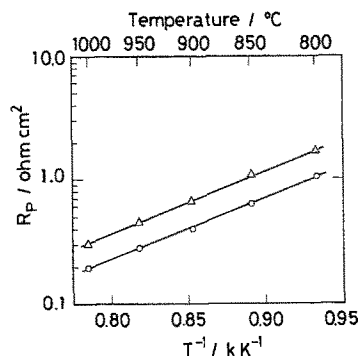


Fig. 5. Arrhenius plot of  $R_p \cdot P_{O_2}$  in the cathode gas (atm);  $\circ$ : 1.0,  $\Delta$ :  $8.36 \times 10^{-2}$ .

The relation between  $\log R_p$  and  $\log P_{O_2}$  is linear in the  $P_{O_2}$  range examined and the gradient is about  $-1/4$  ( $R_p \propto P_{O_2}^{-1/4}$ ). Fig. 5 shows the plot of  $\log R_p$  against  $1/T$  for the platinum cathode. The activation energy is about  $96 \text{ kJ mol}^{-1}$  ( $0.99 \text{ eV}$ ), being independent of the  $P_{O_2}$  at the cathode.

The anodic and cathodic polarization phenomena have been studied at some noble metal electrodes on solid oxide electrolytes [1–18]. Depending on the electrode material, the preparation method of the electrodes and their morphology, various results have been reported. In the fuel cell operation mode, the anodic overpotential seems to be significant, whereas the polarization loss at the cathode (air electrode) is in general not so large. However, when gas with relatively low  $P_{O_2}$  is used, the cathodic overpotential becomes significant due to the diffusion limitation of oxygen molecules or oxygen atoms.

Sasaki *et al.* [15] have investigated the electrode process of the stabilized zirconia cell ( $O_2 + 4e \rightleftharpoons 2O^{2-}$ ) by a complex impedance method. In their studies, the resistance of the electrode reaction ( $R_r$ ) was found to be proportional to  $P_{O_2}^{-1/4}$  for platinum electrodes and it was indicated that the rate determining step (rds) would be (a) the dissociation of oxygen molecules into atoms, (b) the surface diffusion of adsorbed oxygen atoms ( $O(\text{ad})$ ) or (c) the charge transfer step ( $O(\text{ad}) + 2e \rightarrow O^{2-}$ ).

Wang and Nowick [1–4] have studied electrode polarization on doped ceria. For the fine platinum paste electrodes, they showed that the electrode polarization was controlled by charge transfer [1]. In their experiment, the exchange current  $I_0$  was proportional to  $P_{O_2}^{-1/4}$  above  $600^\circ C$  and the acti-

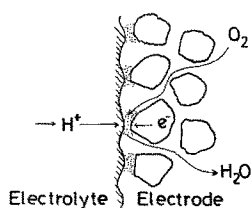


Fig. 6. Schematic illustration of the cathode reaction in the  $H_2$ -fuel cell using proton conductor.

vation energy from  $I_0$  against  $1/T$  was 0.99 eV. They found that oxygen for the charge transfer process was supplied from adsorbed oxygen atoms on the platinum electrode surface which obey the Langmuir isotherm. However, except when the electrode particles were extremely small, the diffusion of oxygen atoms along the electrode was rate determining ( $I_0 \propto P_{O_2}^{3/8}$ ) [4]. A similar conclusion to that of Wang and Nowick [4] has been reported by Verkerk and Burggraaf [6], although the dependence of the electrode resistance ( $R_r$ ) upon  $P_{O_2}$  was somewhat different.

In the present study, the cathodic overpotential was observed at the platinum electrode on a proton conductive solid electrolyte. Similar to the case of the oxide ion conductor cell, in the fuel cell using the proton conductor, oxygen atoms must diffuse into the electrochemically active site, where protons which have migrated across the electrolyte would react with oxygen atoms and electrons ( $2H^+ + 1/2O_2 + 2e \rightarrow H_2O$ ). Schematic illustrations of the electrode reactions and possible elementary steps are shown in Fig. 6 and Table 1. Although the overall cathodic reaction is different from that in the oxide ion conductor cell, some analogous discussion on the transport process of oxygen (Steps 1–3 in Table 1) at the cathode may be possible also in our proton conductor fuel cell.

The value of  $n$  in the form of  $R_p \propto P_{O_2}^{-n}$  characteristics of each rate determining step, is also given in Table 1 [15]. If Step 1 is rate determining,  $R_p$  should be proportional to  $P_{O_2}$  ( $n = 1$ ). From the experimental results obtained above,  $n$  is not unity. So, this diffusion process of oxygen molecules among the electrode particles is considered not to be the rds. When Step 2 is the rds and the adsorption of oxygen obeys the Langmuir isotherm,  $n$  should take values from 1 to 0. Similarly,  $n$  should take values from 1/2 to 0 when Step 3 or

Table 1. Elementary reaction steps at the cathode and value of  $n$  in  $R_p \propto P_{O_2}^{-n}$

Reaction step	$n$ in $R_p \propto P_{O_2}^{-n}$
(1) $O_2(g) \rightarrow O_2(ad)$	1
(2) $O_2(ad) \rightarrow 2O(ad)$	$1 - \theta$
(3) Surface diffusion of $O(ad)$	$1/2 - \theta$
(4) $O(ad) + 2H^+ + 2e \rightarrow H_2O(ad)$	$1/2 - \theta$
(5) $H_2O(ad) \rightarrow H_2O(g)$	0

Overall:  $2H^+ + 1/2O_2(g) + 2e \rightarrow H_2O(g)$ .

4 is the rds. On the other hand, when the diffusion of water vapour produced (Step 5) is rds,  $R_p$  should not depend upon  $P_{O_2}$  ( $n = 0$ ). For Steps 2–4,  $n$  can be estimated rigorously if the surface coverage of oxygen atoms,  $\theta_{ads}$ , is known. Several investigators have discussed the meaning of  $n$  (in  $I_0$  against  $P_{O_2}^n$  or  $R_r$  against  $P_{O_2}^{-n}$ ) [1, 4, 6, 17] assuming  $1 - \theta_{ads} \approx 1$ . According to their reports,  $n$  was 1/4 when charge transfer ( $O(ad) + 2e \rightarrow O^{2-}$ ) was the rds, whereas  $n$  was 3/8 or 1/2 when the surface diffusion of  $O(ad)$  (Step 3 in Table 1) was the rds. However, in our proton conductor fuel cell, water vapour formed at the cathode must be taken into consideration, and since  $\theta_{ads}$  for the platinum electrode in the presence of water vapour is still unclear, we adopt the expression as in Table 1.

In this study,  $n$  was found to be 1/4. Then, either one of the steps from 2 to 4 may be the rds. Verkerk showed that, if Step 3 is the rds, the activation energy  $E_a$  of  $R_p$  is given by  $E_a = \Delta H_d - n\Delta H_{ads}$  where  $\Delta H_d$  and  $\Delta H_{ads}$  are the activation energy for surface diffusion and the heat of adsorption, respectively [6]. Lewis and Gomer [26] found a surface diffusion enthalpy of 1.48 eV for oxygen atoms on platinum at  $T > 500$  K. From this value and our activation energy  $E_a = 0.99$  eV,  $\Delta H_{ads}$  is calculated to be 1.96 eV, which is close to the value in the literature [6, 17]. For the charge transfer step (Step 4), the situation should be different from that in the oxide ion conductor cell. In spite of using different kinds of solid electrolytes (proton and oxide ion),  $n$  is 1/4 (or around 1/4) in both cases. This suggests that the rds for the platinum electrode may be the surface diffusion of adsorbed oxygen atoms toward the electrochemically active site on the solid electrolyte.

#### 4. Conclusion

The polarization phenomena of a SrCeO<sub>3</sub>-based proton conducting solid electrolyte fuel cell were studied using platinum as electrode and hydrogen as a fuel.

The resistance of the solid electrolyte was a major factor in the voltage drop of this cell. While the polarization of the anode was negligibly small, the polarization of the cathode could not be neglected in this experimental condition.

The polarization resistance,  $R_p$ , at the cathode was evaluated and the dependence of the  $R_p$  upon the  $P_{O_2}$  or the temperature were studied. It was found that the  $R_p$  was proportional to  $P_{O_2}^{-1/4}$  and the activation energy was 0.99 eV, similar to the previous results reported for the oxide ion conductor cell. It was suggested that the rate determining step for the cathode reaction was the surface diffusion of adsorbed oxygen atoms on platinum to the electrochemically active site on the solid electrolyte.

#### Acknowledgement

We would like to thank the Ministry of Education, Science and Culture of Japan for supporting part of this work by a grant from the Special Research Project on the Effective Use of Energy (320).

#### References

- [1] D. Y. Wang and A. S. Nowick, *J. Electrochem. Soc.* **126** (1979) 1155.

- [2] *Idem, ibid.* **126** (1979) 1166.  
 [3] *Idem, ibid.* **127** (1980) 113.  
 [4] *Idem, ibid.* **128** (1981) 55.  
 [5] D. Braushtein, D. S. Tannhauser and I. Riess, *ibid.* **128** (1982) 82.  
 [6] M. J. Verkerk, M. W. J. Hammink and A. J. Burggraaf, *ibid.* **130** (1983) 70.  
 [7] M. V. Verkerk and A. J. Burggraaf, *ibid.* **130** (1983) 78.  
 [8] S. V. Karpachov, A. T. Filyayev and S. F. Palgayev, *Electrochim. Acta* **9** (1964) 1681.  
 [9] T. Takahashi, H. Iwahara and I. Ito, *Denki Kagaku* **38** (1970) 288.  
 [10] *Idem, ibid.* **38** (1970) 509.  
 [11] T. H. Etsell and S. N. Flengas, *J. Electrochem. Soc.* **118** (1971) 1890.  
 [12] B. G. Ong, C. C. Chiang and D. M. Manson, *Solid State Ionics* **3/4** (1981) 447.  
 [13] P. Fabry and M. Kleitz, *J. Electroanal. Chem.* **57** (1974) 165.  
 [14] T. M. Gur, I. D. Raistrick and R. A. Huggins, *J. Electrochem. Soc.* **127** (1980) 2620.  
 [15] J. Sasaki, J. Mizusaki, S. Yamauchi and K. Fueki, *Bull. Chem. Soc. Jpn* **54** (1981) 1688.  
 [16] S. P. S. Badwall and H. J. de Bruin, *J. Electrochem. Soc.* **129** (1982) 1921.  
 [17] H. Okamoto, G. Kawamura and T. Kudo, *Electrochim. Acta* **28** (1983) 379.  
 [18] T. Takahashi and H. Iwahara, *Energy Convers.* **19** (1971) 105.  
 [19] H. Iwahara, T. Esaka, H. Uchida and N. Maeda, *Solid State Ionics* **3/4** (1981) 359.  
 [20] H. Iwahara, H. Uchida and T. Esaka, *Prog. Batteries Solar Cells* **4** (1982) 279.  
 [21] H. Iwahara, H. Uchida and N. Maeda, *J. Power Sources* **7** (1982) 293.  
 [22] H. Iwahara, H. Uchida and S. Tanaka, *Solid-State Ionics* **9/10** (1983) 1021.  
 [23] H. Uchida, N. Maeda and H. Iwahara, *J. Appl. Electrochem.* **12** (1982) 645.  
 [24] H. Iwahara, H. Uchida and J. Kondo, *ibid.* **13** (1983) 365.  
 [25] H. Iwahara, H. Uchida and N. Maeda, *Solid-State Ionics* **11** (1983) 109.  
 [26] R. Lewis and R. Gomer, *Surf. Sci.* **12** (1968) 157.